第 28 卷第 12 期 无 机 化 学 学 报 Vol.28 No.12
2012 年 12 月 CHINESE JOURNAL OF INORGANIC CHEMISTRY 2548-2557

不同模拟体液中水化硅酸三钙固化体的体外生物活性行为

倪亚茹*,[1] 林 青[2] 董 亚[1] 陆春华[1] 兰祥辉[1] 许仲梓*,[1]
([1]南京工业大学材料科学与工程学院材料化学工程国家重点实验室,南京 210009)
([2]金陵科技学院材料工程学院,南京 211169)

摘要: 研究水了化硅酸三钙(Ca_3SiO_5,C_3S)固化体的体外生物活性行为。结果表明,干 C_3S 固化体中含有 23.97wt%的 $Ca(OH)_2$,$Ca(OH)_2$ 的溶解导致模拟体液(Simulated Body Fluids, SBF)的 pH 值上升;磷灰石颗粒优先诱导沉积于 C_3S 固化体表面,随后碳酸钙和磷灰石颗粒共同沉积于 C_3S 固化体表面;HCO_3^-是 SBF 模拟体液内主要的缓冲离子;$Ca(OH)_2$ 碳化和 $CaCO_3$ 沉积主要导致 SBF 的 pH 值下降。由于离子交换作用的减弱,C_3S 固化体表面最终被磷灰石完全覆盖, 磷灰石的沉积促使 SBF 的 pH 值进一步降低。因此,对于 C_3S 和其衍生材料的体外生物活性和生物相容性必须考虑到 HCO_3^-在体内的实际含量和行为。

关键词: 体外生物活性; 硅酸三钙; 磷灰石; 碳酸钙
中图分类号: O614.23+1 **文献标识码**: A **文章编号**: 1001-4861(2012)12-2548-10

In Vitro Bioactive Behaviors of Hydrated Tricalcium Silicate Paste in Different Simulated Body Fluids

NI Ya-Ru*,[1] LIN Qing[2] DONG Ya[1] LU Chun-Hua[1] LAN Xiang-Hui[1] XU Zhong-Zi*,[1]
(*State Key Laboratory of Materials-Orient Chemical Engineering, College of Materials Science and Engineering, Nanjing University of Technology, Nanjing* 210009, *China*)
([2]*School of Material Engineering, Jinling Institute of Technolgy, Nanjing* 211169, *China*)

Abstract: The *in vitro* bioactive behaviors of hydrated tricalcium silicate (Ca_3SiO_5, C_3S) paste were studied. The results show that dry hydrated C_3S paste contains about 23.97wt% $Ca(OH)_2$, and the dissolution of $Ca(OH)_2$ results in increased pH value of simulated body fluid (SBF). Apatite particles are firstly induced to deposit on hydrated C_3S paste surface. Then, hydrated C_3S paste surface is co-deposited with $CaCO_3$ and apatite particles. HCO_3^- is the principal buffer system of SBF, and the carbonation of $Ca(OH)_2$ and deposition of $CaCO_3$ mainly contribute to the decreasing of pH value. As a result of lower ion exchanges, hydrated C_3S paste surface is finally deposited with apatite. The deposition of apatite contributes to the further decreasing of pH value. The *in vitro* bioactivity and further biocompatibility evaluations of C_3S and C_3S devised materials must be improved by considering the concentration and behavior of HCO_3^- in living body.

Key words: *in vitro* bioactivity; tricalcium silicate; apatite; calcium carbonate

The therapeutic effects of bioactive glasses arise from the influences of soluble Ca and Si ions on the gene expression of osteoprogenitor cells[1-2]. The key to design the new bioactive Ca-Si-based materials is to control the dissolution concentrations of Ca and Si ions[2]. Thus, the development of bioactive Ca-Si-based materials with the self-setting property is feasible and desired[3-5]. C_3S based cements have been developed to

收稿日期:2012-12-20。收修改稿日期:2012-05-08。
国家 973 计划(2009CB623105)、南京市医学科技发展重点项目(ZKX07016)和江苏省研究生创新基金项目(CX09B-127Z)资助项目。
*通讯联系人。E-mail:nyr@njut.edu.cn(倪亚茹); zzxu@njut.edu.cn(许仲梓)

circumvent the shortcomings of traditional Ca-Si-based bioactive materials[4]. Tricalcium silicate (Ca_3SiO_5, C_3S) has been extensively studied as novel bone cements for dental and orthopaedic surgery[3], because of its excellent self setting property, bioactivity, degradability and stimulation effect on cell growth[5-7]. The excellent self setting property of C_3S could be described by the following idealized hydration reaction.

$$Ca_3SiO_5+(3+y-x)H_2O=$$
$$xCaO\cdot SiO_2\cdot yH_2O+(3-x)Ca(OH)_2 \quad (1)$$

As with other Ca-Si-based bioactive materials, an essential requirement for C_3S bone cement is the bioactivity. The bioactivity is often evaluated by examining the deposition ability of apatite on the material surface in a simulated body fluid (SBF) with the ion concentrations nearly to those of human blood plasma (Table 1)[8]. There is wide consensus that hydrated C_3S paste could induce the deposition of apatite in SBF[5]. However, the deposition of apatite on hydrated C_3S paste has not been fully clarified. Because, four factors are underestimated or ignored:

(1) The present and the content of $Ca(OH)_2$ in hydrated C_3S paste;

(2) HCO_3^- concentration in SBF is lower than that in human blood plasma (Table 1);

(3) The carbonation of $Ca(OH)_2$ by incorporating HCO_3^- from SBF;

(4) The deposition relationships between apatite and $CaCO_3$.

Table 1　Ion concentrations of human blood plasma, SBF, P-SBF and C-SBF

Type	Ion concentration / (mmol·L^{-1})							
	Na^+	K^+	Mg^{2+}	Ca^{2+}	Cl^-	HCO_3^-	HPO_4^{2-}	SO_4^{2-}
Human blood plasma	142.0	5.0	1.5	2.5	103.0	27.0	1.0	0.5
SBF solution	142.0	5.0	1.5	2.5	147.8	4.2	1.0	0.5
P-SBF solution	137.8	5.0	1.5	2.5	147.8	0	1.0	0.5
C-SBF solution	142.0	3.0	1.5	2.5	147.8	4.2	0	0.5

So, the further investigation of *in vitro* bioactivity of hydrated C_3S paste is necessary and useful as an initial and basic study of C_3S bone cement. For this purpose, the composition and structure of anhydrous C_3S and hydrated C_3S paste were characterized. Furthermore, we try to approach the problems by studying the *in vitro* bioactive behaviors of hydrated C_3S paste in different SBFs.

1　Experimental

1.1　Preparation of materials

C_3S powder was prepared by the solid state reaction as previous described[9]. C_3S powder was mixed with deionized water with a liquid to powder (L/P) ratio of 0.5 mL·g^{-1} to form a homogenous mixture. Then, the mixture was stirred and stored at 37 ℃ and 100% relative humidity for 24 h to form the hydrated C_3S paste.

1.2　Characterization of materials

Hydrated C_3S paste was transferred into ethanol, and dried in a vacuum for 24 h. Anhydrous C_3S powder and dry hydrated C_3S paste were characterized by X-ray diffraction (XRD; ARL XTRA, Thermo Electron, America), Fourier transform infrared spectroscopy (FTIR; Nexus 670, Nicolet, America) and ^{29}Si solid state magic angle spinning nuclear magnetic resonance (^{29}Si MAS NMR; Avance 400D, Bruker, Germany). XRD patterns were recorded with Cu $K\alpha$ radiation (λ=0.154 18 nm) at 36 kV and 30 mA. The scanning speed was kept at 10°·min^{-1} with a step-scan interval of 0.02°. FTIR spectra were collected using a KBr pellet method with a resolution of 2 cm^{-1} and a scan number of 32. ^{29}Si MAS NMR studies were conducted under a magnetic field strength of 7.0455 T and a ^{29}Si resonance frequency of 59.63 MHz. Samples were packed in 7 mm zirconia rotors and spun at 5 kHz under an angle of 54°44′. The chemical shifts were recorded relative to external tetramethylsilane (TMS). A thermal analyzer (Sta449C, Netzsch, Germany) was used to conduct thermogravimetric

analysis and differential thermal analysis (TG-DTA) of hydrated C_3S paste. Hydrated C_3S paste was examined from 50 to 1 000 ℃ with a heating rate of 10 ℃·min^{-1}.

1.3 *In vitro* bioactivity

SBF was prepared according to the procedures described by Kokubo [8]. Comparing with SBF, P-SBF and C-SBF were prepared without the addition of $NaHCO_3$ and $K_2HPO_4·3H_2O$ (Table 1), respectively. Hydrated C_3S pastes were soaked in SBF, P-SBF and C-SBF with a surface area-to-volume ratio of 0.1 cm^{-1} at 37 ℃ for 3 d. The solutions were refreshed by 12 h. The pH values of SBF, C-SBF and P-SBF before refreshing on the 12th hour were measured by an electrolyte-type pH meter (pHS-2S, Leici, Shanghai, China). At the given time, hydrated C_3S pastes were gently rinsed with deionized water followed by drying at room temperature. Hydrated C_3S paste surfaces were characterized by XRD (ARL XTRA, Thermo Electron, America) with the same condition as above. The morphological variations of paste surfaces were characterized by SEM (JSM-5900, JEOL, Tokyo, Japan) equipped with an energy dispersive X-ray spectrometer (EDX, Thermo Electron, USA). SEM micrographs were taken using an acceleration voltage of 5.0 kV. EDS spectra were performed with an accelerating voltage of 1 kV for the electron beam (beam current 2 nA) using a data collection time of 1 00 s.

2 Results and discussion

2.1 Characterization of materials

Fig.1 shows the XRD patterns of anhydrous C_3S powder and hydrated C_3S paste. Anhydrous C_3S powder undergoes a hydration reaction and transforms to hydrated C_3S paste, which consists of crystalline $Ca(OH)_2$ and amorphous C-S-H gel.

Fig.2 shows the FTIR spectra of anhydrous C_3S powder and hydrated C_3S paste. The peaks of anhydrous C_3S powder at 931~808, 520 and 449 cm^{-1} are attributed to Si-O stretching [10]. In the spectrum of hydrated C_3S paste, the partially resolved doublet peaks at 1 430 and 1 480 cm^{-1} are attributed to

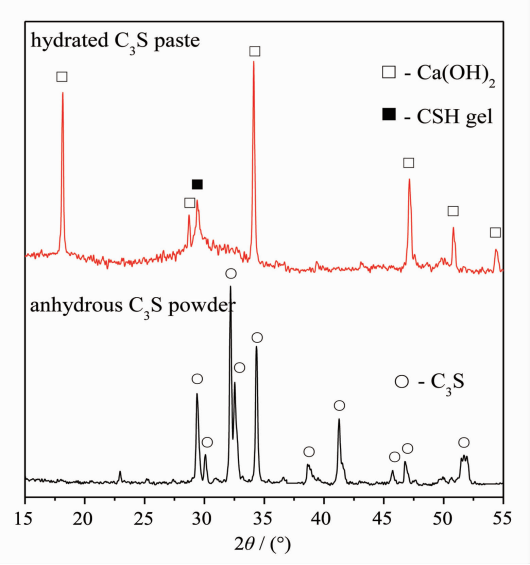

Fig.1 XRD patterns of anhydrous C_3S powder and hydrated C_3S paste

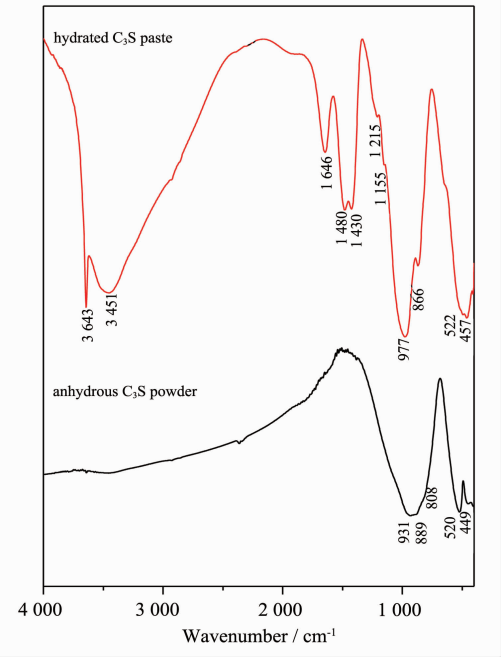

Fig.2 FTIR spectra of anhydrous C_3S powder and hydrated C_3S paste

carbonate species for the reaction of $Ca(OH)_2$ with atmospheric CO_2. The stretching mode of O-H in $Ca(OH)_2$ gives rise to a sharp signal at 3 643 cm^{-1}[10]. The characteristic peak at 977 cm^{-1} indicates the polymerization and formation of C-S-H gel in hydrated C_3S paste[11].

^{29}Si MAS NMR spectra of anhydrous C_3S powder and hydrated C_3S paste are shown in Fig.3. Gaussian

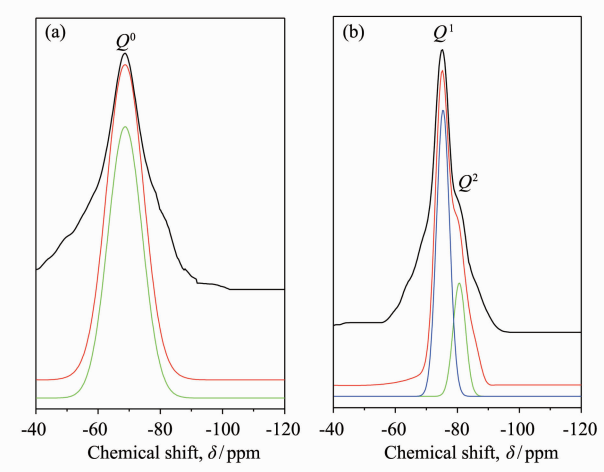

Fig.3　^{29}Si MAS NMR spectra of anhydrous C_3S powder (a) and hydrated C_3S paste (b)

peak deconvolution is employed to separate and quantify Q^n units with peak positions adopted from extensive studies [12]. Anhydrous C_3S raises a single resonance at −68.67 ppm (Fig.3a). It indicates that silicate tetrahedrons ([SiO_4]) are isolated in the crystal structure of C_3S[13]. In turn, peaks located at −80.75 and −75.22 ppm correspond to Q^1 and Q^2 units in C-S-H gel [14]. Moreover, the mean silicate chain length ($\overline{CL}$) of C-S-H gel in hydrated C_3S paste is about 3.35, which was calculated from the intensity of Q^1 and Q^2 units (Fig.3b) according to the following equation[14].

$$\overline{CL} = \frac{2}{(\frac{Q^1}{Q^1+Q^2})} \tag{2}$$

Two important quantities are obtained from TG-DTA curves of hydrated C_3S paste in Fig.4. First, the chemically bound water is defined as the mass loss due to the decomposition between 140 ℃ (the boiling temperature of free water in the paste) and 1 000 ℃, which can be understood as the amount of water needed for C_3S to hydration[15]. The mass at 140 ℃ is defined as the total mass of the dry hydrated C_3S paste. As a result the chemical bond water completely loses at 1 000 ℃, the mass at 1000 ℃ is regarded to be equal to the mass of original anhydrous C_3S (MCa_3SiO_5). The second mass loss corresponds to the decomposition of $Ca(OH)_2$, which occurs between 440 and 520 ℃[15]. The masses at 105, 440, 520 and 1 000 ℃ (T_{105}, T_{440}, T_{520} and T_{1000}) are listed in Table 2.

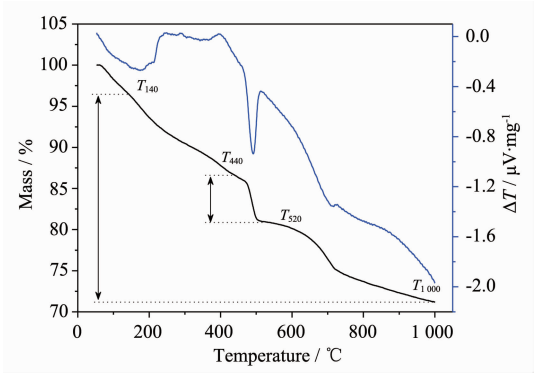

Fig.4　TG-DTA curves of hydrated C_3S paste

Consequently, $Ca(OH)_2$ content in hydrated C_3S paste (W_{CH}), x and y in Eq.(**1**) can be simply calculated as following.

$$W_{CH} = \frac{m_{Ca(OH)_2}\cdot(T_{440}-T_{520})}{m_{H_2O}\cdot T_{140}}\times 100\% = \frac{74(T_{440}-T_{520})}{18T_{140}}\times 100\% \approx 23.97\text{wt}\% \tag{3}$$

$$n_{CaO} = \frac{3M_{Ca_3SiO_5}}{m_{Ca_3SiO_5}} - \frac{T_{440}-T_{520}}{m_{H_2O}} = \frac{3T_{1000}}{m_{Ca_3SiO_5}} - \frac{T_{440}-T_{520}}{m_{H_2O}} = \frac{3T_{1000}}{228} - \frac{T_{440}-T_{520}}{18} \tag{4}$$

$$n_{SiO_2} = \frac{M_{Ca_3SiO_5}}{m_{Ca_3SiO_5}} = \frac{T_{1000}}{m_{Ca_3SiO_5}} = \frac{T_{1000}}{228} \tag{5}$$

$$n_{H_2O} = \frac{(T_{140}-T_{1000})-(T_{440}-T_{520})}{m_{H_2O}} = \frac{(T_{1105}-T_{1000})-(T_{440}-T_{520})}{18} \tag{6}$$

$$x = \frac{n_{CaO}}{n_{SiO_2}} \approx 2.00 \tag{7}$$

$$y = \frac{n_{CaO}}{n_{SiO_2}} \approx 3.52 \tag{8}$$

Where,

$m_{Ca(OH)_2}$=molecular weight of $Ca(OH)_2$=74;

$m_{Ca(OH)_2}$=molecular weight of water=18;

$m_{Ca(OH)_2}$=molecular weight of C_3S=228.

Dry hydrated C_3S paste contains about 23.97wt% $Ca(OH)_2$, and the chemical formula of C-S-H gel could be expressed as $2.00CaOSiO_2\cdot 3.52H_2O$.

2.2　pH values

$Ca(OH)_2$ in hydrated C_3S paste is a strong alkaline substance with a pH value of 12.50 and shows various biological properties and antibacterial

Table 2 Analysis data form the TG-DTA curves

Sample	T_{140} /%	T_{440} /%	T_{520} / %	T_{1000} /%	W_{CH} /wt%	Chemical formula of C-S-H gel
Hydrated C_3S paste	96.58	86.60	80.97	71.18	23.97	$2.00CaO \cdot SiO_2 \cdot 3.52H_2O$

effects [12]. However, release of OH^- from $Ca(OH)_2$ contribute to the increased pH value of the neighboring tissue, which may be detrimental to cell and tissue [16]. Human blood plasma or SBF has a buffering ability due to the presences of HPO_4^{2-} and HCO_3^- (Table 2). In contrast to the previous in vitro studies [4-5], P-SBF and C-SBF were devised as references to compare with the *in vitro* bioactivity in SBF (Fig.5).

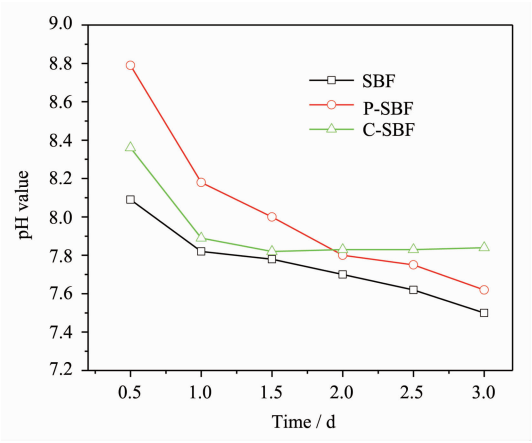

Fig.5 pH values of SBF, P-SBF and C-SBF soaked with hydrated C_3S pastes

The original pH values of SBF, P-SBF and C-SBF are 7.40. After 12 hours of soaking, P-SBF has the highest pH value than SBF and C-SBF. The pH value variations of P-SBF and C-SBF soaking with hydrated C_3S pastes indicate the buffering effects of HPO_4^{2-} and HCO_3^- (Fig.5), respectively. HCO_3^- is conventionally described as the principal buffer system of blood plasma. However, the pH value of C-SBF finally maintain at about 7.80. In contrast, the deposition of apatite would contribute a continue decreasing of pH value of P-SBF. The continuous decreasing of pH value suggests that the biocompatibility of hydrated C_3S pastes would be improved with increased soaking time (Fig.5).

2.3 XRD patterns

After 3 days of soaking in SBF, the diffraction peaks of $CaCO_3$ completely disappear, and the characteristic peaks of apatite become the main constituent of the pattern (Fig.6a). The peaks of apatite are detected on hydrated C_3S paste surface after soaking in P-SBF for 1 day, and become the main constituent of the pattern after soaking for 3 days (Fig.6b). During the whole soaking processes, only the peaks of crystalline $CaCO_3$ are detected on hydrated C_3S paste surfaces soaking in C-SBF (Fig. 6c).

2.4 SEM micrographs

After soaking in SBF and P-SBF for 2 hours, hydrated C_3S paste surfaces are completely deposited with the ball-like particles (Fig.7d and e). Although

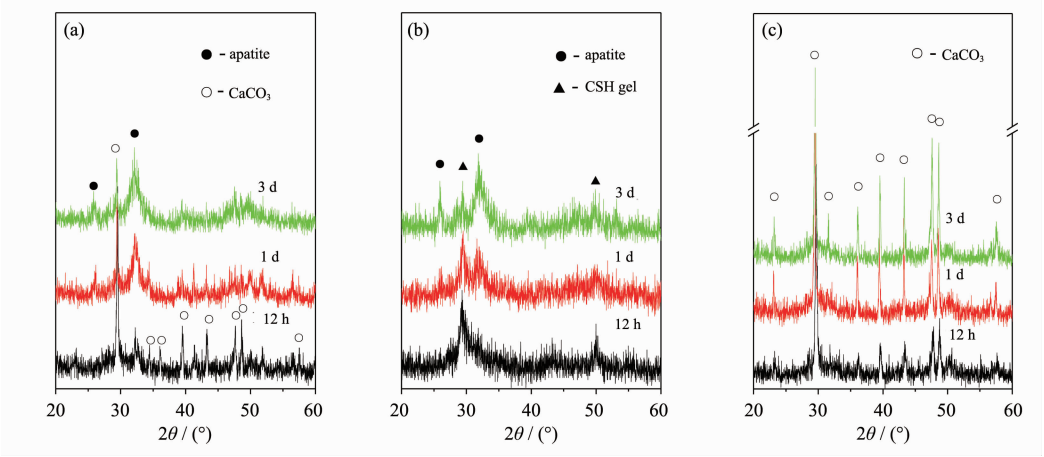

Fig.6 XRD patterns of hydrated C_3S paste surfaces soaked in SBF, P-SBF and C-SBF

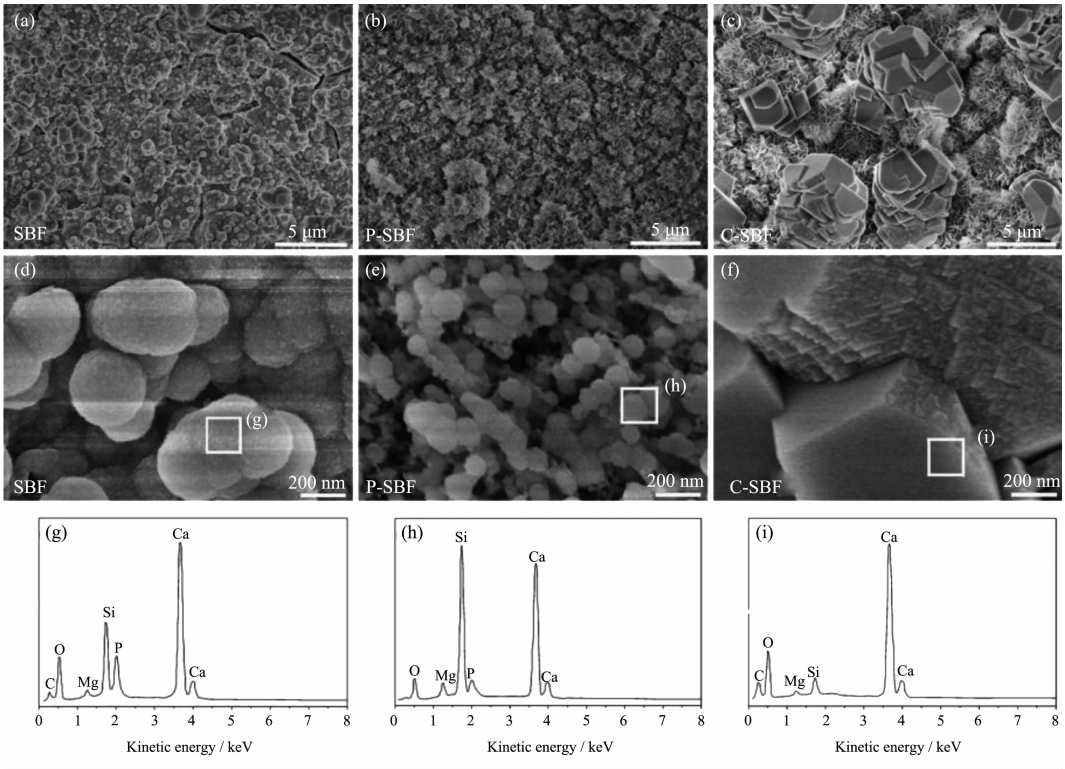

Fig.7　SEM images and EDS spectra of hydrated C_3S paste surfaces soaked in SBF, P-SBF and C-SBF for 2 h

EDS spectra indicate the particles are composed of Ca and P elements (Fig.7g and h), the particles on the hydrated C_3S paste surface soaked in SBF are larger than those in P-SBF. Moreover, the carbon element content of the particles on hydrated C_3S paste surface soaked in SBF are higher than those in P-SBF (Fig.7g and h). In contrast, the large irregular particles, which are constructed with relative small cube-like particles, sporadically deposit on hydrated C_3S paste surface soaked in C-SBF. Because there are no HPO_4^{2-} in C-SBF, EDS spectrum confirms that the particles are consisted of $CaCO_3$ (Fig.7i).

The relative large (Fig.8a) and small (Fig.8d) ball-like particles deposit on hydrated C_3S paste surface soaked in SBF for 12 hours. As it is reported previous [4-5,10], the large particles are consisted of $CaCO_3$ which is attributed to the carbonization of Ca $(OH)_2$ by incorporating HCO_3^{2-} form SBF (Fig.8a). Hydrated C_3S paste surface soaked in P-SBF is deposited with apatite particles (Fig.8b), which have a lager size than those on hydrated C_3S paste surface soaked in SBF. Irregular $CaCO_3$ particles deposit on hydrated C_3S paste surface soaked in C-SBF (Fig.8c and f). The edge and surface of $CaCO_3$ particles are distorted, and the growth steps of the particle edges are observable (Fig.8f).

Hydrated C_3S paste surfaces soaked in SBF and P-SBF for 3 d have the same characterization (Fig.9a and b), the flake-like apatite layers deposited on their surfaces, and these could be confirmed by the XRD results (Fig.6a and b). Hydrated C_3S paste surface soaked in C-SBF for 3 d are still deposited with $CaCO_3$ particles (Fig.9c).

2.5 *In vitro* bioactive behaviors

^{29}Si MAS NMR spectra demonstrate that the isolated silicate tetrahedrons ($[SiO_4]$) of anhydrous C_3S polymerized to form C-S-H gel with a chain structure during the hydration process (Fig.3). C-S-H gel presents a layered structure based on Ca-O sheets ribbed with linear silicate "dreierketten" chains (Fig. 10). It is clear that the special structure of C-S-H gel (Fig.10) could provide favorable sites (Si-OH) for apatite nucleation and deposition. The deposition of apatite particles on hydrated C_3S paste soaked in P-SBF accords to the following reaction.

$$10Ca^{2+}(aq)+6HPO_4^{2-}(aq)+8OH^-(aq) =$$

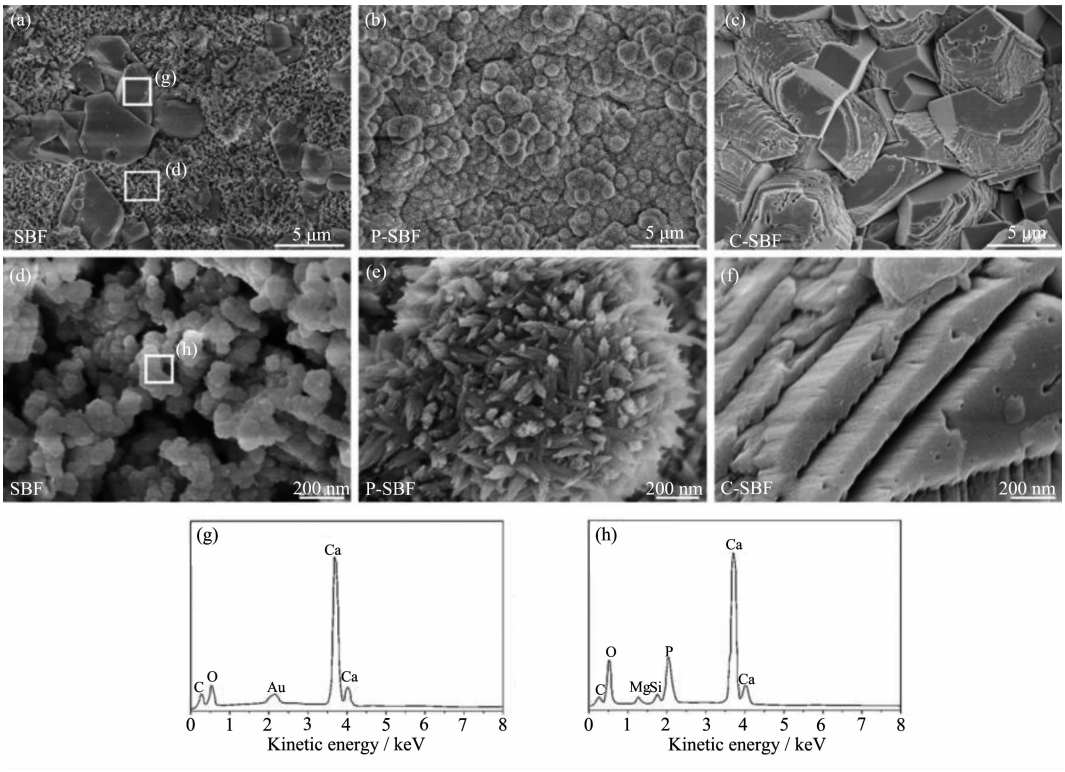

Fig.8 SEM images of hydrated C_3S paste surfaces soaked in SBF, P-SBF and C-SBF for 12 h

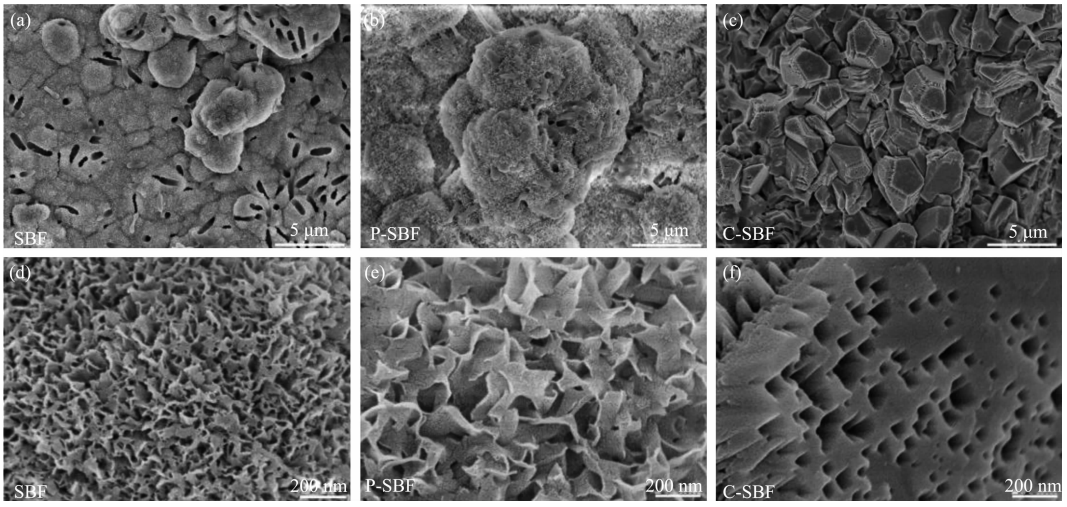

Fig.9 SEM images of hydrated C_3S paste surfaces soaked in SBF, P-SBF and C-SBF for 3 d

$$Ca_{10}(PO_4)_6(OH)_2(s)+6H_2O(l) \quad (\mathbf{9})$$

Then, apatite particles grow spontaneously, and consume HPO_4^{2-} from the refreshing P-SBF. The HCO^{3-} in C-SBF (Table 1) and Ca $(OH)_2$ in hydrated C_3S paste (Table 2) are favorable for the carbonation of Ca $(OH)_2$ and deposition of $CaCO_3$ (Fig.7c). The deposition of $CaCO_3$ is directly attributed to the carbonation of Ca $(OH)_2$ by incorporating HCO_3^- form C-SBF [Eq.(**10**)].

$$Ca^{2+}(aq)+OH^-(aq)+HCO_3^-(aq) = CaCO_3(s)+H_2O(l) \quad (\mathbf{10})$$

It is easy to understand that hydrated C_3S paste soaked in SBF is deposited with both apatite and $CaCO_3$ particles. Thus the solubility product (K_{SP}) of apatite [$\lg K_{SP}$=117.2 for $Ca_{10}(PO_4)_6(OH)_2$] is lower than that of $CaCO_3$ ($\lg K_{SP}$=8.48 for calcite)[17-18], hydrated C_3S paste surface may sustain the earlier nucleation and deposition of apatite particles than that of $CaCO_3$

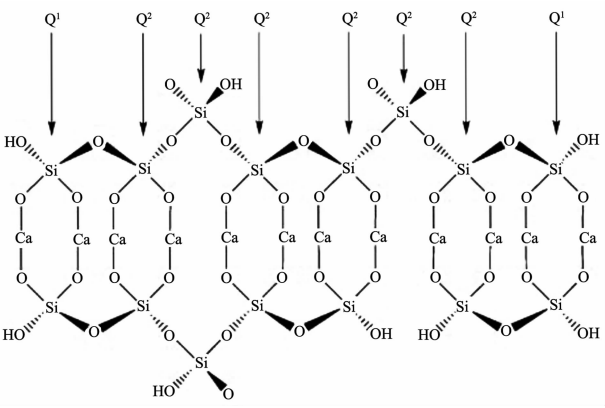

Layer of seven-fold coordinated Ca is sandwiched in between "dreierketten" chain of silicate tetrahedron ([SiO_4])

Fig.10　Schematic representation of the basic structure of the C-S-H gel

particles (Fig.7d). Therefore, it is observed that hydrated C_3S paste surface is deposited with apatite particles after soaking in SBF for 2 h without the appearance of $CaCO_3$ particles (Fig.7d). EDS results also prove that apatite particles deposited on hydrated C_3S paste surface soaked in SBF contains more carbon element than that in P-SBF (Fig.7g and h). It means that the deposition of B-type carbonated apatite (HCA) [Eq. (**11**)] is more kinetically favorable than the deposition of stoichiometric apatite [$Ca_{10}(PO_4)_6(OH)_2$] on hydrated C_3S paste surface soaked in SBF[19].

$$(10-0.5x)Ca^{2+}(aq)+6HPO_4^{2-}(aq)+xHCO_3^-(aq)+8OH^-(aq)=Ca_{10-0.5x}(PO_4)_6(CO_3)_x(OH)_2\ (s)+6H_2O(l) \quad (\mathbf{11})$$

The fabrication of apatite seeds would serve as the new sites for the nucleation and growth of apatite and $CaCO_3$. After soaking in SBF for 12 h, hydrated C_3S paste surface is deposited with the relative large $CaCO_3$ particles and small apatite particles (Fig.8a). As the result of high solubility product of $Ca(OH)_2$ (lgK_{SP}=5.32 for portlandite)[20] and the consumption of $Ca(OH)_2$ by deposition of apatite and $CaCO_3$ particles, $Ca(OH)_2$ could not be detected in XRD (Fig.6). As the result of lowed ion exchanges between hydrated C_3S paste and SBF weakened by apatite and $CaCO_3$ layer, the deposition of $CaCO_3$ would be stopped. On the other hand, $CaCO_3$ is a metastable phase in SBF as compared with apatite, the deposited $CaCO_3$ may partly converse to apatite in term of a dissolution-precipitation process [21]. Therefore, hydrated C_3S paste surface is finally deposited with apatite after soaking in SBF for 3 days (Fig.9a).

Based on above comparative studies, the *in vitro* bioactivity of hydrated C_3S paste in SBF is further clarified as following stages (Fig.11).

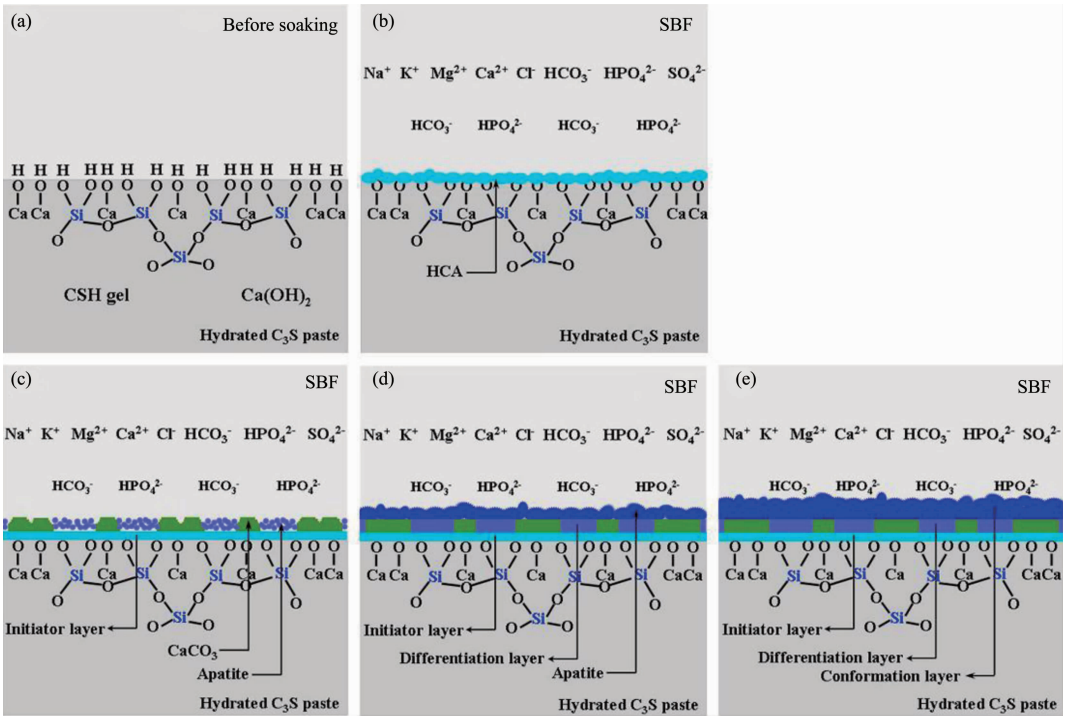

Fig.11　Schematic presentations of process of apatite deposition on hydrated C_3S paste surface soaked in SBF

Stage I. When anhydrous C_3S powders react with water, C-S-H gel and $Ca(OH)_2$ are the main hydration products of hydrated C_3S paste. The polymerization and solidification of C-S-H gel contributes the setting and strength of hydrated C_3S paste, which exposes a surface with a flake-like morphology before soaking (Fig.8 in Ref. [4]).

Stage II. The dissolution of $Ca(OH)_2$ with the releases of Ca^{2+} and OH^- results in increased pH value of SBF (Fig.5). The nucleation and deposition of B-type carbonated apatite (HCA) is triggered by silanol (Si-OH) groups of C-S-H gel, which act as the nucleation sites (Fig.7a). B-type carbonated apatite layer is defined as the initiator layer (Fig.9b).

Stage III. A new layer composed of large crystalline $CaCO_3$ particles and small apatite particles is formed and referred as the differentiation layer (Fig. 11c). The pH value of SBF continues to decreasing as the result of the consumption of Ca^{2+} and OH^-. $Ca(OH)_2$ on the surface of hydrated C_3S paste would completely dissolve into Ca^{2+} and OH^- and transform to $CaCO_3$ and apatite.

Stage IV. The initiator and differentiation layers restrain the ion exchanges between hydrated C_3S paste and SBF, the deposition of $CaCO_3$ particles is ended. Apatite particles deposit by consuming Ca^{2+} and HPO_4^{2-}, which are mainly form the refreshing SBF. This new apatite layer is named as the conformation layer (Fig.11d).

Stage V. Hydrated C_3S paste surface is finally deposited with apatite layer. As the result that the ion exchanges between hydrate C_3S paste surface and SBF are in dynamic equilibrium, the pH value of SBF is stable at 7.40.

In this study, HCO_3^- is closely related to the carbonation of $Ca(OH)_2$ and deposition of $CaCO_3$ on hydrated C_3S paste surface. Human blood plasma has lower Cl^- and higher HCO_3^- concentrations (27.0 mmol·L^{-1}) than SBF (Table 1). It is speculated that the carbonation of $Ca(OH)_2$ and deposition of $CaCO_3$ would be enhanced on hydrated C_3S paste surface in living body. The bioactivity and biocompatibility would be significantly influenced by HCO_3^-. So, the ionic dissolution products of hydrated C_3S paste *in vitro* would be far from that of hydrated C_3S paste *in vivo*. It means that cell proliferation assay of hydrated C_3S paste can not be directly predicted from the results of traditional method[7,22]. As the conditions of the in vitro bioactivity and biocompatibility described in the literatures have not yet been standardized, it is crucial and a challenge to precisely specify HCO_3^- concentration during the experiments. By feeding these data back, it would be possible to assist the rational design and improvement processes of C_3S and C_3S derived materials.

3 Conclusions

The *in vitro* bioactive behaviors of hydrated C_3S paste are clarified in this study. C-S-H gel and $Ca(OH)_2$ are the main hydration products of C_3S. The isolated silicate tetrahedrons in anhydrous C_3S polymerized to form C-S-H gel with a layered structure based on Ca-O sheets ribbed with linear silicate chains. There is about 23.97wt% $Ca(OH)_2$ in dry hydrated C_3S paste, the dissolution of $Ca(OH)_2$ results in increased pH value of SBF. Apatite particles are firstly induced to deposition on hydrated C_3S paste surface. Then, hydrated C_3S paste surface are co-deposited with $CaCO_3$ and apatite particles. HCO_3^- is the principal buffer system of SBF, and the carbonation of $Ca(OH)_2$ and deposition of $CaCO_3$ mainly contribute to the decreasing of pH value. As the result of lowed ion exchanges, hydrated C_3S paste surface is finally deposited with apatite. The deposition of apatite contributes to the further decreasing of pH value. Because HCO_3^- concentration of SBF is lower than that of human blood plasma, the carbonation and deposition of $CaCO_3$ on hydrated C_3S paste would be enhanced in living body. The concentrations and behaviors of HCO_3^- must be emphasized and recognized during the bioactivity and biocompatibility studies of C_3S and C_3S devised materials.

References:

[1] Hench L L. *J. Eur. Cer. Soc*., **2008**,**29**(7)1257-1265

[2] Christodoulou I, Buttery L D, Saravanapavan B P, et al. *J. Biomed. Mater. Res*., **2005**,74B(1):529-537

[3] Gandolfi M G, Pagani S, Perut P, et al. *J. Biomed. Mater. Res*., **2008**,**87**A(2):477-486

[4] Lin Q, Lan X, Li Y, et al. *Mater. Sci. Eng. C*, **2010**,**31**(3): 629-636

[5] Zhao W, Wang J, Wang Z, et al. *Biomaterials*, **2005**,**26**(31): 6113-6121

[6] Zhao W, Chang J. *Mater. Sci. Eng. C*, **2007**,**28**(2):289-293

[7] Laurent P, Camps I, De Meo M, et al. *Dent. Mater*., **2008**,**24** (11):1486-1494

[8] Kokubo T, Takadama H. *Biomaterials*, **2006**,**27**(15):2907-2915

[9] Lin Q, Li Y, Lan X, et al. *Biomed. Mater.*, **2009**,**4**:045005

[10]Coleman N J, Awosanya K, Nicholson J W, et al. *J. Biomed. Mater. Res*., **2008**,**90**(1):166-174

[11]Mollah M Y A, Yu W, Schennach R, et al. *Cem. Con. Res*., **2000**,**30**(2):267-273

[12]Narita H, Itoh S, Imazato S, et. al. *Acta Biomater.*, **2010**,**6** (2):586-590

[13]Tran T T, Herfort D, Jakobsen H J, et. al. *J. Amer. Chem. Soc*., **2009**,**13**1(40):14170-14171

[14]Richardson L G. *Cem. Con. Res*., **1999**,**29**(8):1131-1147

[15]Pane I, Hansen W. *Cem. Con. Res*., **2005**,**35**(6):1155-1164

[16]Wu C, Ramaswamy Y, Soeparto A, et. al. *Biomed. Mater. Res*., **2008**,**86**A(2):402-410

[17]Ren D, Feng Q. *Bourrat X, Micron*, **2010**,**42**(3):228-245

[18]Muler L, Muler F A. *Acta Biomater*., **2006**,**2**(2):181-189

[19]Lu X, Leng Y. *Biomaterials*, **2005**,**26**(10):1097-1108

[20]Wen Y, Xiang L, Jin Y, et al. *Mater. Let*., **2003**,**57** (16): 2565-2571

[21]Guo Y, Zhou Y, Jia D, et al. *Micropor. Mesopor. Mater.*, **2009**,**118**(2):480-488

[22]Huang Y, Jin X, Zhang X, et al. *Biomaterials*, **2009**,**30**(28): 5041-5048